ELSEVIER

Journal of Hydrology 216 (1999) 17–31

Journal of Hydrology

Tidal effects on sea water intrusion in unconfined aquifers

B. Ataie-Ashtiani[a], R.E. Volker[b,*], D.A. Lockington[b]

[a]*Department of Civil Engineering, Sharif University of Technology, Tehran, Iran*
[b]*Department of Civil Engineering, University of Queensland, Queensland 4072, Australia*

Received 17 November 1997; accepted 19 October 1998

Abstract

A variable-density groundwater model is used to analyse the effects of tidal fluctuations on sea-water intrusion in an unconfined aquifer. It is shown that the tidal activity forces the sea-water to intrude further inland and it also creates a thicker interface than would occur without tidal effects. Moreover, the configuration of the interface is radically changed when the tidal fluctuations are included. This is because of the dramatic changes in the flow pattern and velocity of the groundwater near the shoreline. For aquifer depths much larger than tidal amplitudes, the tidal fluctuation does not have much effect on how far the sea-water intrudes into the aquifer; nevertheless, a significant change in the configuration of concentration contours because of the effect of tidal fluctuations is observed. This change is more noticeable at the top of the aquifer, near the water table, than at the bottom of the aquifer, and is caused by the infiltration of salt water into the top of the aquifer at higher tidal levels. A flatter beach slope, therefore, intensifies this phenomenon. The interface configurations do not change noticeably over the course of a tidal cycle. Neglecting tidal fluctuation effects results in an inaccurate evaluation of the water table elevation at the land end of the aquifer, although no distinguishable difference is seen between the water tables near the shoreline. Where the landward boundary condition is a constant head, the effects of tidal fluctuations on sea-water intrusion are more pronounced than for cases where the landward boundary condition is a specified flux. Also it is shown that the effects of tidal fluctuations are more significant for a sloping beach than for a vertical shoreline and the salt water intrudes further inland for the sloping case.

Keywords: Groundwater flow; Coastal aquifer; Sea-water intrusion; Numerical modelling

1. Introduction

When a coastal aquifer discharges fresh groundwater to the sea, an interface or dispersion zone occurs where the fresh water and seawater come into contact. The location, shape and extent of the dispersion zone depend upon several factors including the scale, the shape or the structure of the aquifer, and the parameters such as hydraulic conductivity. Other influential factors are groundwater inflow from the upstream region, as well as groundwater withdrawals through pumping, and the tidal oscillation of the sea level. Philip (1973) and Smiles and Stokes (1976) for the first time pointed out that, even for zero net discharge to sea, the nonlinear influence of a sinusoidal tidal motion on a vertical shoreline will cause the water table to rise above mean sea level; this elevation of the water table is called overheight herein. Nielsen (1990) developed an analytical solution to the one-dimensional Boussinesq equation for the sloping beach case. In this model it is assumed that water table oscillations die out far from the beach, and decoupling between the water table and the tide does not occur. The first assumption is a reasonable

* Corresponding author; e-mail: ataie@civil.sharif.ac.ir

0022-1694/99/$ - see front matter
PII: S0022-1694(98)00275-3

approximation for many beaches, while the second assumption is probably too simple, as during the ebb period the exit point is often decoupled from the sea level and a seepage face is formed. Although analytical solutions are simple and instructive for those cases where decoupling does not occur, they are not sufficient for predicting the behaviour of a dynamic exit point and seepage face and, therefore, for predicting the full water table and groundwater dynamics. Analytical models are also limited by assuming: a uniform thickness of aquifer above an impermeable layer underlying the beach; a constant beach face angle; a uniform hydraulic conductivity and specific yield; and, a single inland boundary condition at which water table oscillations reduce to zero. Moreover all of the analytical solutions are based on the assumption that the water in the aquifer is a single phase homogenous fluid. To overcome these limitations, numerical methods are needed. Numerical modelling of this problem, with the assumption of a single density fluid, has been done by Fang et al., (1972), Li et al., (1997), Volker et al. (1997).

The salt-water intrusion phenomenon in groundwater systems has been conceptualised by two general approaches: the sharp interface approach and the dispersed interface approach. In the former it is assumed that the salt-water and freshwater are immiscible fluids separated by a sharp interface. In the latter a transition zone of mixed salt and fresh water is considered to be present at the interface. In this approach, the diffusion and hydrodynamic dispersion effects, density dependent fluid flow and solute transport are incorporated. An historical perspective of salt-water intrusion is presented by Reilly and Goodman (1985). The models of Volker (1980), who employed the finite element method for the saltwater intrusion problems in coastal confined and unconfined aquifers, Volker and Rushton (1982), Taigbenu et al., (1984) who applied the boundary integral method, and the models of Mercer et al. (1980), Polo and Ramis (1983), Ledoux et al. (1990), who used the finite difference method are based on the first approach.

Custodio (1988) mentions that in many real situations, such as sluggish freshwater flow, stresses caused by tidal oscillations and recharge events, and enhanced dispersivity by macroscopic heterogeneities, this approach is a crude one. Moreover, the concentration of dissolved solids cannot be predicted by these models. The impact of these limitations is clear when considering that water of potable quality contains less than about one percent seawater (Voss and Souza, 1987).

Numerical models based on the dispersed interface approach have been used extensively to investigate different aspects of sea-water intrusion by including the density difference between sea-water and fresh groundwater (Segol et al., 1975; Volker and Rushton, 1982; Frind, 1982; Voss and Souza, 1987; Konikow and Arevalo, 1993). However, there has not been much work done on including tidal fluctuations in the sea water intrusion problem.

The effects of tide on the groundwater lens dynamics on atoll islands were investigated by Hogan (1988) and Underwood et al. (1992) using the SUTRA model (Voss, 1984). In their works they did not consider a real free surface water table. Inouchi et al. (1990) presented an approximate analytical solution and a numerical model for analysing seawater intrusion in a confined aquifer including the effects of tide.

The present study investigates the effect of tide on sea-water intrusion in unconfined aquifers and the consequences of both these factors for the groundwater table. Such a study has not been attempted previously perhaps because of the complexities of the problem, such as solving the water table free surface, simulating density dependent miscible fluid flow at the sea boundary, and handling complex boundary conditions like tidal fluctuations along the mild slope of beaches. Also in order to model the transient behaviour of groundwater in response to tidal oscillations a very short time step should be applied and this causes a need for enormous computational effort.

The groundwater behaviour in an unconfined aquifer with a mild sloping face in response to a tide is affected by two factors that do not exist in a confined aquifer. These factors are the infiltration of salt water from the top of the beach slope into the aquifer at high tide and tidal pumping with a free water table. The latter effect is intensified by a mild sloping beach and the existence of a seepage-face at the sea boundary of the groundwater.

The objectives of this article are to investigate the effects of tidal fluctuation on sea-water intrusion in an unconfined aquifer and the effects of both of these together on groundwater dynamics.

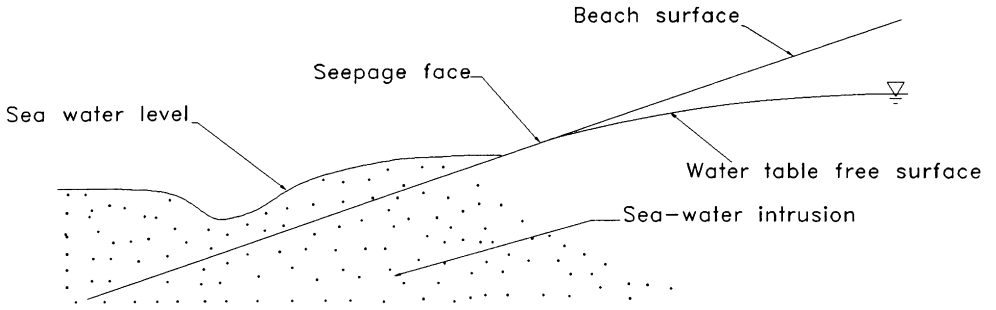

Fig. 1. Conceptual model of the relationship between groundwater and sea.

2. Numerical model

To simulate groundwater flow in an unconfined coastal aquifer including the detailed effects of the sea boundary condition, a numerical model should have three capabilities. First, it should be able to solve the water table free surface problem. Second, the numerical model should be able to simulate salt-water intrusion and therefore density dependent miscible fluid flow at the sea boundary. Third, it should be able to handle complex boundary conditions like tidal fluctuations along the mild slope of beaches, which sometimes cause a long seepage face at the beach (Fig. 1).

Solving the water table free surface problem can be done either by solving the equation for water movement in variably saturated porous media, or by neglecting the unsaturated zone and solving the groundwater flow equation in the saturated part and adjusting the water table by some numerical techniques. Although the first approach requires greater computational effort, it represents more realistically the actual situation; moreover in cases where the capillary fringe and unsaturated zone play a significant role it is essential for an accurate result.

SUTRA (Voss, 1984) is chosen as the basis for numerical modelling in this work because of its ability to solve density dependent and variably saturated flow. This model was also readily available in source code form.

It implements a hybridisation of finite element and integrated finite difference methods employed in the framework of a method of weighted residuals. In this model, standard finite-element approximations are employed only for terms in the balance equations which describe fluxes of fluid mass, solute mass and energy. All other non-flux terms are approximated with a finite element mesh version of the integrated finite difference methods.

In the work reported here SUTRA has been improved for modelling of groundwater flow and contaminant transport in an unconfined coastal aquifer by three changes. First, in order to enhance the ability of the model to handle variably saturated flow, the basic two-dimensional variably saturated flow equation has been changed from pressure form to a mixed form. The mixed form of the general variably saturated flow equation is solved using the modified Picard iteration scheme presented by Celia et al. (1990).

Second, to improve the abilities of the model to accommodate the nonlinearity of the unsaturated equation, an automatic under-relaxation method is applied in calculating the pressure after each iteration.

Third, the model has also been adjusted to handle a seepage face boundary condition which is important, especially in cases where there is a large amplitude tidal fluctuation on beaches of mild slope.

SUTRA had been validated by comparison with Henry's solution and the results of Elder (1967) for a problem of complex natural convection (Voss, 1984; Voss and Souza, 1987) and successfully applied to solve real problems (Voss and Souza, 1987). After the above mentioned modifications, the modified version of SUTRA was validated by the experimental data of Vauclin et al. (1975) to test its ability to provide accurate solutions for problems with a seepage face. In addition the experimental results of Ataie-Ashtiani (1998) were used to validate the model for simulation of groundwater flow in response to the

periodic boundary condition in unconfined aquifers with a mild sloping face.

3. Mathematical formulations

The governing equation describing the SUTRA fluid mass balance, was written in pressure-based form as (Voss, 1984)

$$\frac{\partial}{\partial x_i}\left[\frac{k_{ij}k_r\rho}{\mu}\left(\frac{\partial p}{\partial x_j}-\rho g e_j\right)\right] = \left(S_w\rho S_{op}+\varepsilon\rho\frac{dS_w}{dp}\right)\frac{\partial p}{\partial t}+\varepsilon S_w\frac{\partial p}{\partial c}\frac{\partial c}{\partial t}-Q_p, \quad (1)$$

where p is pressure; c is solute concentration of fluid as a mass fraction; k_{ij} is the permeability tensor; k_r is the relative permeability with respect to the water phase; $x_i (i=1,2)$ are Cartesian coordinates; t is time; e_j is the unit gravitational vector in the direction of x_2 (assumed to be vertically upward); Q_p is fluid mass source; S_w is degree of saturation; S_{op} is the specific pressure storativity; ρ is fluid density; μ is fluid viscosity; ϵ is porosity; and g is gravitational acceleration.

In this work SUTRA was modified to solve the mixed form of the variably saturated flow equation

$$\frac{\partial}{\partial x_i}\left[\frac{k_{ij}k_r\rho}{\mu}\left(\frac{\partial p}{\partial x_j}-\rho g e_j\right)\right] = S_w\rho S_{op}\frac{\partial p}{\partial t}+\varepsilon\rho\frac{dS_w}{dt}+\varepsilon S_w\frac{\partial\rho}{\partial c}\frac{\partial c}{\partial t}-Q_p. \quad (2)$$

The modified Picard iterative procedure for the mixed form of the variably saturated flow equation is fully mass conserving in the unsaturated zone. In contrast, conventional, pressure-based formulations exhibit poor mass-based formulations exhibit poor mass-balance behaviour (Celia et al., 1990).

The van Genuchten (1980) soil water equations are used for unsaturated soil hydraulic properties

$$S_w=\left[\frac{1}{1+[a|h|]^n}\right]^m, \quad (3a)$$

$$k_r(S_w)=S_w^{(1/2)}[1-(1-s_w^{1/m})^m]^2, \quad (3b)$$

in which h is pressure head and a, n, and m are fitting parameters, with m related to n by $m=1-1/n$. Degree of saturation is defined as $(\theta-\theta_r)/(\theta_s-\theta_r)$, where θ is water content and θ_r and θ_5 are residual and saturated water contents.

Solute transport is simulated through numerical solution of a solute mass balance equation including advective and dispersive spreading mechanisms. This is described mathematically by:

$$\varepsilon\rho\frac{\partial c}{\partial t}+\varepsilon p v_i\frac{\partial c}{\partial x_i}-\frac{\partial}{\partial x_j}\left[\varepsilon\rho(D_m\delta_{ij}+D_{ij})\cdot\frac{\partial c}{\partial x_i}\right] = Q_p(c^*-c), \quad (4)$$

where v_i is fluid velocity, D_{ij} is the mechanical dispersion tensor, D_m is the molecular diffusion coefficient of the solute in pure fluid including aquifer material tortuosity effects, c^* is concentration of solute as a mass fraction in the source fluid, and δ_{ij} is equal to 1 if $i=j$, otherwise it is zero.

Density is given as a linear function of concentration:

$$\rho=\rho_0+\frac{\partial p}{\partial c}(c-c_0), \quad (5)$$

where ρ_0 is fluid density at the reference solute concentration $c=c_0$.

Darcy's law gives the mass average fluid velocity at any point in a cross section as

$$v=-\frac{\partial}{\partial x_i}\left[\frac{k_{ij}k_r}{\varepsilon\mu}\left(\frac{\partial\rho}{\partial x_j}-\rho g e_j\right)\right]. \quad (6)$$

The dispersion tensor, $\underline{D}$, is expressed for a two dimensional system as:

$$\underline{D}=\begin{bmatrix}D_{11} & D_{12}\\ D_{21} & D_{22}\end{bmatrix}, \quad (7)$$

where $\underline{D}$ is symmetric and the diagonal elements are:

$$D_{11}=\left(\frac{1}{v^2}\right)(d_L v_1^2+d_T v_2^2), \quad (8)$$

$$D_{22}=\left(\frac{1}{v^2}\right)(d_T v_1^2+d_L v_2^2) \quad (9)$$

and the off-diagonal elements are:

$$D_{12}=D_{21}=\left(\frac{1}{v^2}\right)(d_L-d_T)(v_1 v_2). \quad (10)$$

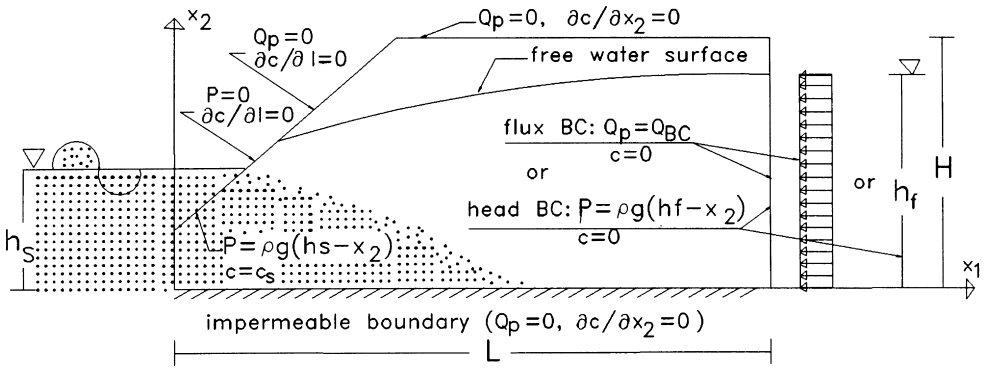

Fig. 2. Schematic of the flow domain and boundary conditions (BC) used in the simulations.

The term d_L and d_T are called the longitudinal and transverse dispersion coefficients, respectively.

The size of the dispersion coefficients in an isotropic flow system depend upon the absolute magnitude of the average velocity in a flowing system (Bear, 1979):

$$d_L = \alpha_L v, \tag{11a}$$

$$d_T = \alpha_T v, \tag{11b}$$

where α_L and α_T are the longitudinal and transverse dispersivities, respectively.

The general expressions for flow boundary conditions are given by

$$p(x_i, t) = p_{BC} \text{ on } B_1, \tag{12a}$$

$$Q_p = Q_{BC} \text{ on } B_2, \tag{12b}$$

where B_1 is the portion of the flow boundary where p is prescribed as p_{BC}, B_2 is portion of the flow boundary where the fluid mass source is prescribed as Q_{BC}.

Another type of flow boundary condition that is considered is the seepage face. A seepage-face is an external boundary of the saturated zone where flux is directed outward and there is atmospheric pressure along that boundary. Negative pressures exist above the seepage-face within the porous medium. Therefore, atmospheric pressure is maintained for all the nodes along the seepage-face and they are treated as Dirichlet nodes with the prescribed pressure, $p = 0$. Nodes above the seepage face are specified as no-flow nodes. The position of the seepage-face is initially unknown and constitutes a non-linear boundary condition. Hence, the seepage face must be determined using an iterative process.

For the transport equation, the boundary conditions take the form

$$c(x_i, t) = c_{BC} \text{ on } B'_1, \tag{13a}$$

$$\frac{\partial c}{\partial 1} = 0 \text{ on } B'_2, \tag{13b}$$

$$Q_P = Q_{BC}, c^* = c^*_{BC} \text{ on } B'_3, \tag{13c}$$

where B'_1 is the portion of the boundary where concentration is prescribed as c_{BC}, B'_2 is the portion of the boundary where the convective flux in the direction normal to the boundary is the same on both sides of the boundary, 1 is the outward normal at the boundary, and B'_3 is the portion of the boundary where a known flux at a known concentration, c_{BC}*, enters the system.

4. Problem description

A schematic representation of the basic problem is presented in Fig. 2. The coastal aquifer ($L = 180$ m long and $H = 10$ m deep with a 1 : 10 beach slope) has no-flow boundaries on the base of the flow domain. For this study the influence of rainfall is assumed to be very small as a short domain length has been considered, and therefore a no flow boundary was used for the top of the flow domain. The seaward boundary is described by a mean sea water level of $h_s = 7$ m, on which is superimposed a sinusoidal

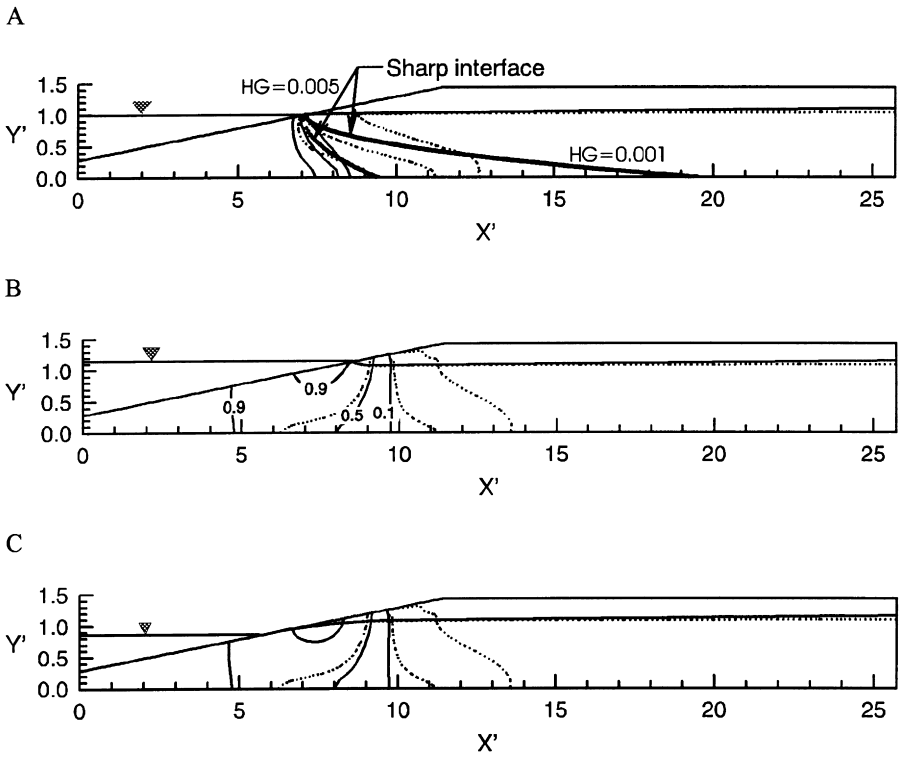

Fig. 3. (a) Steady-state, (b) high tide, (c) low tide salt concentration contours, 0.1, 0.5 and 0.9, in cases where the landward boundary condition is a specific flux with the hydraulic gradient (HG) values of 0.005 (solid line) and 0.001 (dotted line).

semidiurnal tide with amplitude $A = 1$ m and 12 h period. The values of the other parameters used are:

horizontal and vertical saturated hydraulic conductivity $K_h = K_v = 8.4$ m day^{-1};
porosity $\epsilon = \theta_s = 0.3$;
residual water content
$\theta_r = 0.01$;
specific storage
$S_s = 10^{-6}$m^{-1};
Van Genuchten soil parameters
$a = 3.3$ m^{-1}, $n = 4.1$;
longitudinal dispersivity
$\alpha_L = 2$ m;
transverse dispersivity
$\alpha_T = 0.2$ m;
sea-water solute mass fraction
$c_s = 0.036$;
sea-water density
$\rho_s = 1025$ kg m^{-3};
fresh-water density
$\rho_0 = 1000$ kg m^{-3}

And therefore, $\partial\rho/\partial c = 700.3$ kg m^{-3}.In order to interpret the results more easily and to generalise the conclusions of this analysis, the following normalised non-dimensional forms of parameters are considered:

$$X' = x_1/h_s, Y' = x_2/h_s, \alpha_L prime = \alpha_L/h_s, \alpha_T prime = \alpha_T/h_s, A' = A/h_s, c' = c/c_s.$$

Therefore for this problem $\alpha_L{}' = 0.286$, $\alpha_T{}' = 0.029$ and $A' = 0.143$.

The dimensions of the finite element mesh vary from 0.5 m near the seaward boundaries to 5 m in landward parts of the aquifer. A smaller element size is used at the seaward boundaries to model the seepage face and salt concentration more accurately. The numbers of nodes and elements are 1070 and 949

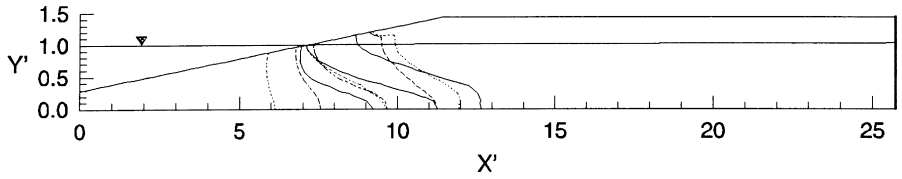

Fig. 4. Salt concentration contours, 0.1, 0.5 and 0.9, in cases where the landward boundary condition is a specified flux with hydraulic gradient value of 0.001 when $\alpha_L{}' = 0.286$, $\alpha_T{}' = 0.029$ (solid line), $\alpha_L{}' = 1.429$, $\alpha_L{}' = 0.029$ (dotted line) and $\alpha_L{}' = 0.286$, $\alpha_L{}' = 0.143$ (broken line).

respectively. Time step, Δt, varies from 0.5 h to 50 h for the cases without tidal fluctuations and is constant at 0.5 h for simulation of tidal effects.

5. Results

The first set of results is obtained for the case where a constant flow is imposed at the landward boundary. The two assumed values for the inflow flux are 4.2×10^{-2} m day^{-1} and 8.4×10^{-3} m day^{-1} which correspond to hydraulic gradients of 0.005 and 0.001, respectively.

Steady-state (without tide case) and transient (with tide case) salt concentration distributions for these cases are shown in Fig. 3, where solid and dashed lines represent isochlor contours computed for

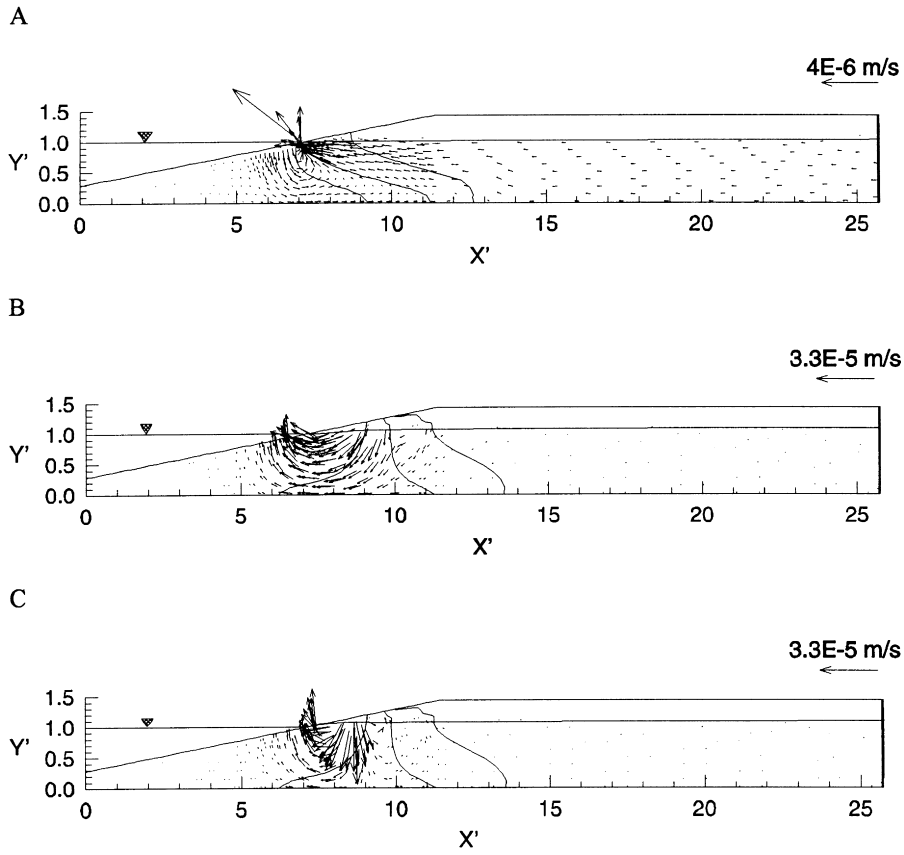

Fig. 5. (a) Steady-state, (b) rising tide from mean sea water level and (c) falling tide from mean sea water level velocity field for the case where the landward boundary condition is a constant flux with hydraulic gradient 0.001.

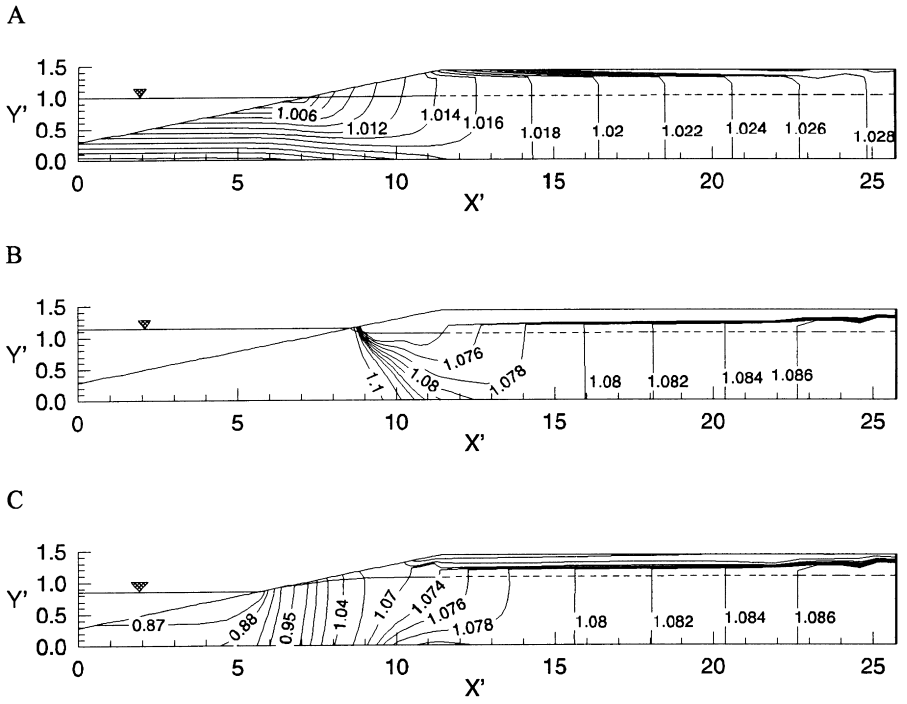

Fig. 6. Steady-state (a), high tide (b) and low tide (c) equipotential lines for the case where the landward boundary condition is a constant flux and hydraulic gradient is 0.001.

hydraulic gradients of 0.005 and 0.001, respectively. The normalised concentration contours 0.1, 0.5, and 0.9 are shown in the figure. The sharp interfaces based on Glover (1959) solution are also shown in Fig. 3a for both hydraulic gradients. The results of the cases without tidal fluctuations (Fig. 3a) show that the seaward fresh-water flux in the aquifer has a considerable influence on both the shape and the location of the interface as was shown by Volker and Rushton (1982) for confined aquifers. Fig. 3a shows that less freshwater discharged to sea not only causes the seawater to intrude further inland, but it also causes the occupied space between 0.1 and 0.9 contours to increase. The 0.1–0.9 contours occupy a space of $1.2h_s$ along the base of aquifer for 0.005 hydraulic gradient case compared to $3.3h_s$ for 0.001 hydraulic gradient case. In other words, it makes the interface more dispersed. As seen, the sharp interface gives a good approximation of the dispersed interface for the case of larger hydraulic gradient, as the interface in this case is thinner than that for the other case. However for the small gradient case, the sharp interface approximation is far from the dispersed solution for the 0.5 contour.

The effects of tidal fluctuation on the interface are observed by comparing the steady-state result with the transient results in Fig. 3. Clearly the tidal activity forces the sea-water to intrude further inland and it also creates a thicker interface. Moreover, the configuration of the interface is radically changed when the tidal fluctuations are included. This is because of the dramatic changes in the flow pattern and velocity of the ground water near the shoreline. The contours do not change noticeably in a tidal cycle, as can be seen by comparing the high tide results (Fig. 3b) with low tide results (Fig. 3c).

When the dispersivities are increased the difference between sharp and dispersed interface solutions becomes more pronounced as one would expect. Fig. 4 illustrates the effects of varying the dispersivity values. Salt concentration contours are shown for cases with other parameters the same as for the 0.001 gradient case in Fig. 3. In one case $\alpha_L{}'$ and in the other case $\alpha_T{}'$ is increased five times to

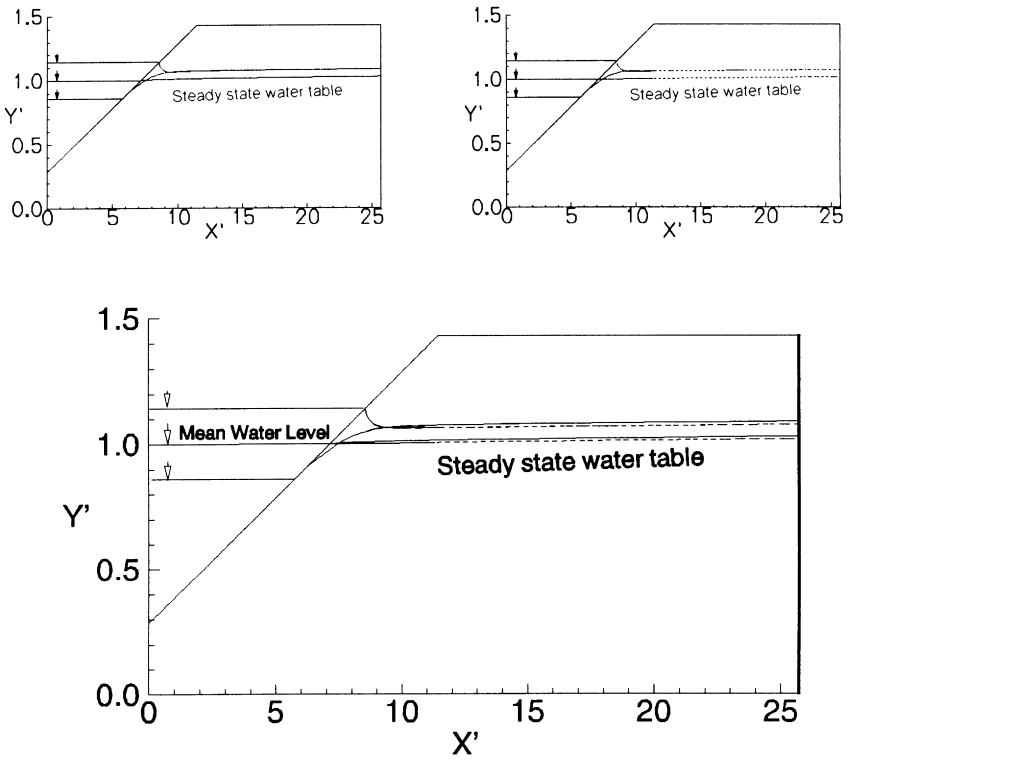

Fig. 7. Water tables predicted for steady-state, high tide and low tide in the cases where the higher density of sea-water is considered (solid line) and neglected (broken line) and where the landward boundary condition is constant flux with hydraulic gradient 0.001.

1.429 and 0.143, respectively. Comparing with Fig. 3a, it is seen that the interface becomes more dispersed and therefore increasingly differs from the sharp interface solution. This figure also shows that the effects of both transverse and longitudinal dispersivity are important for the configuration of the interface, although the interrace configuration is most sensitive to the changes in longitudinal dispersivity.

Fig. 5 shows the velocity field for the steady-state case and also for the rising and falling tide situations when the hydraulic gradient is 0.001. For the steady-state case a circulation of entering salt-water from the beach face and exiting from the exit point exists. However for the transient case, while this circulation of salt-water exists, it is obscured in the figures by another stronger circulation of fresh-water in the immediate vicinity of the shore. The former circulation is caused by the density difference between sea-water and freshwater, while the latter is caused by an over-height in the groundwater table caused by tidal fluctuations, especially in mildly sloping beaches.

Fig. 6 shows the equipotential lines for the steady-state case and the high and low tide stages of the transient case. As seen, the pattern of the equipotential lines near the shoreline in the transient case is very different from that for the steady-state. However, the pattern is the same further inland, except that the value of the equipotential for the line near the upstream end for the transient case is about $0.06h_s$ higher than that for the steady-state case.

To show the effects of higher sea-water density on the response of groundwater level to tidal fluctuations, some results are now presented for cases where different fluid densities are considered. The water table positions for the steady state case and at high and low tide for the fluctuating sea level case are shown in Fig. 7 for situations when the higher sea-water density is considered and when it is neglected. As seen, the water table for the case with tidal fluctuation

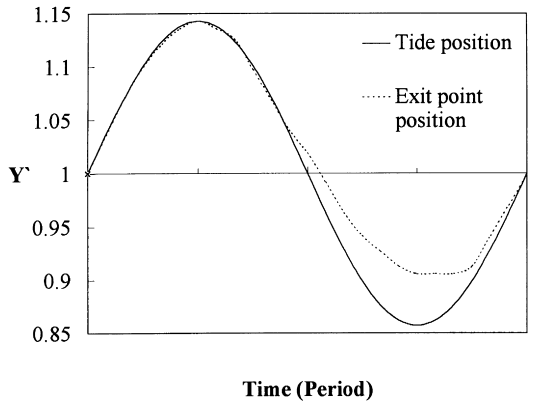

Fig. 8. The elevation of the exit point and the tidal water level over a tidal cycle.

of sea level is higher than the corresponding water table position for the steady sea level case. The water elevations at the landward boundary for the steady-state and transient cases, neglecting the density effects, are $1.019h_s$ and $1.076h_s$. When sea-water density effects are considered, the corresponding elevations are $1.029h_s$ and $1.089h_s$. Neglecting tidal fluctuation effects results in an inaccurate evaluation of the water table in the aquifer. This figure also shows that the effect of sea-water density is to cause higher over-height far in land, although in these cases little difference is seen between the water tables near the shoreline.

The extra over-height estimated by Nielsen (1990) approximate analytical solution for sloping beach and small tidal amplitude is $\zeta A/2$, where ζ is kA cot β. β is the angle that the beach forms with the horizontal and k is the wave number that is given by

$$K = (\pi\varepsilon/KTh_s)^{0.5}. \quad (14)$$

Substituting parameter values for our case in this equation yields an estimated overheight of $0.128h_s$, which is far from the $0.057h_s$ calculated for this case when the density effects of sea-water are neglected. The analytical solution is based on the assumption that the amplitude of fluctuation is much smaller than the depth of aquifer, which is not true for the case

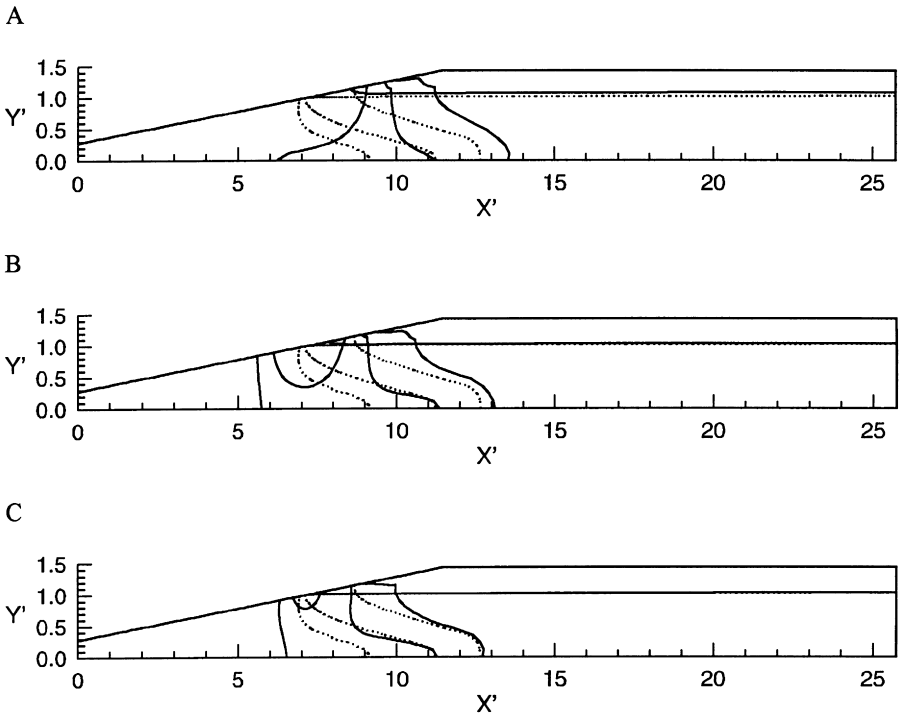

Fig. 9. Water tables and concentration contours predicted for steady-state (dotted line) and high tide (solid line) for (a) $A' = 0.143$, (b) $A' = 0.071$ and (c) $A' = 0.036$ in the case where the landward boundary condition is a constant flux and the hydraulic gradient is 0.001.

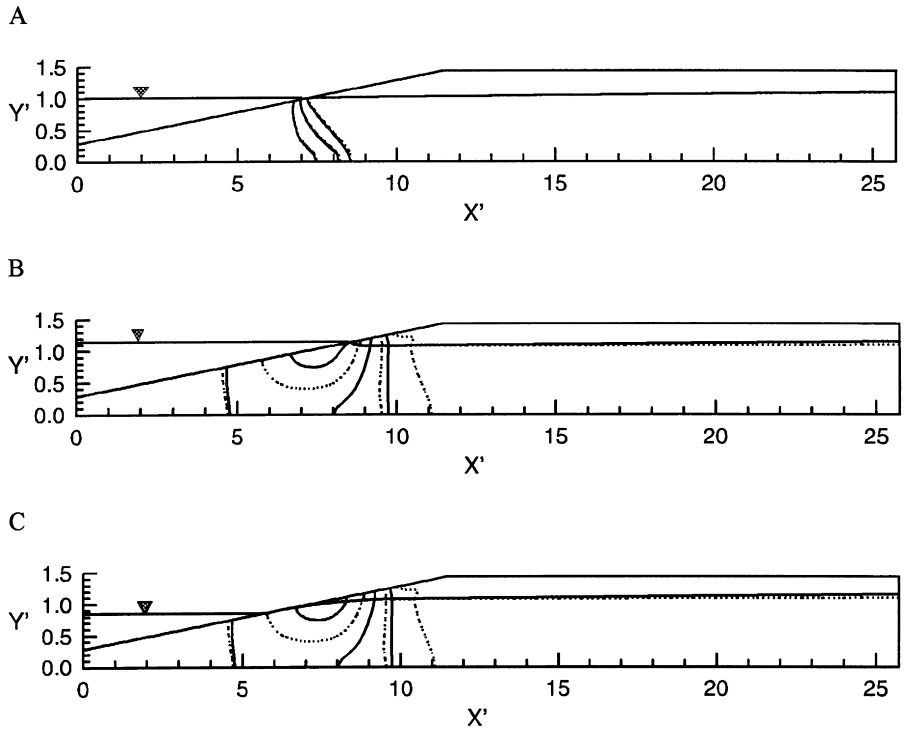

Fig. 10. (a) Steady-state, (b) high tide and (c) low tide water tables and salt concentration contours, 0.1, 0.5 and 0.9, for cases where the landward boundary condition is a constant head of 7.65 m (dotted line) and a constant flux of 4.2×10^{-2}m day^{-1} (solid line), both of these cases representing a 0.005 hydraulic gradient at steady-state condition.

considered here. However some other deficiencies are observed in Nielsen (1990) approximate analytical solution, for example if it is assumed that the beach slope in this case is about 1:11.2 or milder, then the over-height estimated will be larger than the tide amplitude, A, which does not seem reasonable. As the analytical solution is a perturbation solution in ζ, it should be used only for ζ much smaller than 1.

The elevations of both the exit point and the tide are plotted in Fig. 8. It is clear that there is a seepage face during most of the falling tide period and even in the first stages of the rising tide period. For example, the exit point is about $0.049h_s$ above the sea water level at low tide. Neglecting this phenomenon causes an under-estimation of water table elevation.

Obviously, A' is one of the parameters expected to play a role in determining the importance of tidal activity effects on seawater intrusion. Fig. 9 shows the normalised concentration contours 0.1, 0.5, and 0.9 for the high tide stage and the steady-state cases when the A' is 0.143, 0.071 and 0.036. As shown, the effects of tidal fluctuations on sea water intrusion decrease when A' is decreased; for example the distance from the intersection of the sea with the shoreline to the 0.1 contour toe is about $6.6h_s$, $6.1h_s$ and $5.7h_s$ for A' of 0.143, 0.071, and 0.036 respectively, in comparison with $5.6h_s$ for the case without tidal fluctuations. As seen in Fig. 9 for small A', or in other words for aquifer depths much larger than tidal amplitudes, the tidal fluctuation does not have much effect on how far the sea water intrudes into the aquifer. However, even for the smallest value of A' equal to 0.036, a significant change in the configuration of contours caused by the effect of tidal fluctuations is observed.

Fig. 9 also shows that the changes in the configuration of concentration contours caused by the tidal activity are more noticeable at the top of the aquifer, near to the waer table, than at the bottom of the aquifer. This is caused by the infiltration of salt water into

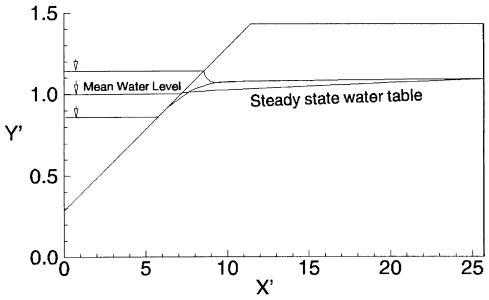

Fig. 11. Water tables predicted for steady-state, high tide and low tide for the case where the landward boundary condition is a constant head of 7.65 m (equivalent to 0.005 hydraulic gradient at steady-state condition).

the top of the aquifer at higher tidal levels and therefore a flatter beach slope intensifies this phenomenon. The other interesting observation based on Fig. 9 is in regard to the position of the 0.5 contour toe. Although the configuration and the toe positions of all contours have changed caused by the tidal fluctuations, a very small change is observed in the position of the 0.5 contour toe.

The water elevations at the landward boundary for these cases are $1.089h_s$, $1.043h_s$, and $1.032h_s$. The over-heights in the groundwater table caused by the tidal fluctuation are about $0.06h_s$, $0.014h_s$, and $0.003h_s$ in these cases.

In those cases where the landward boundary condition is a constant head, for example in the cases where the aquifer extends to a lake or river at the landward boundary, the effects of tidal fluctuations on sea-water intrusion into the aquifer might be stronger. This is because of the reduction in the groundwater flux caused by the over-height in the water table caused by tidal fluctuations. To investigate this possibility, the same problem is solved for cases where a constant head of 7.65 m is imposed at the land boundary (h_f).

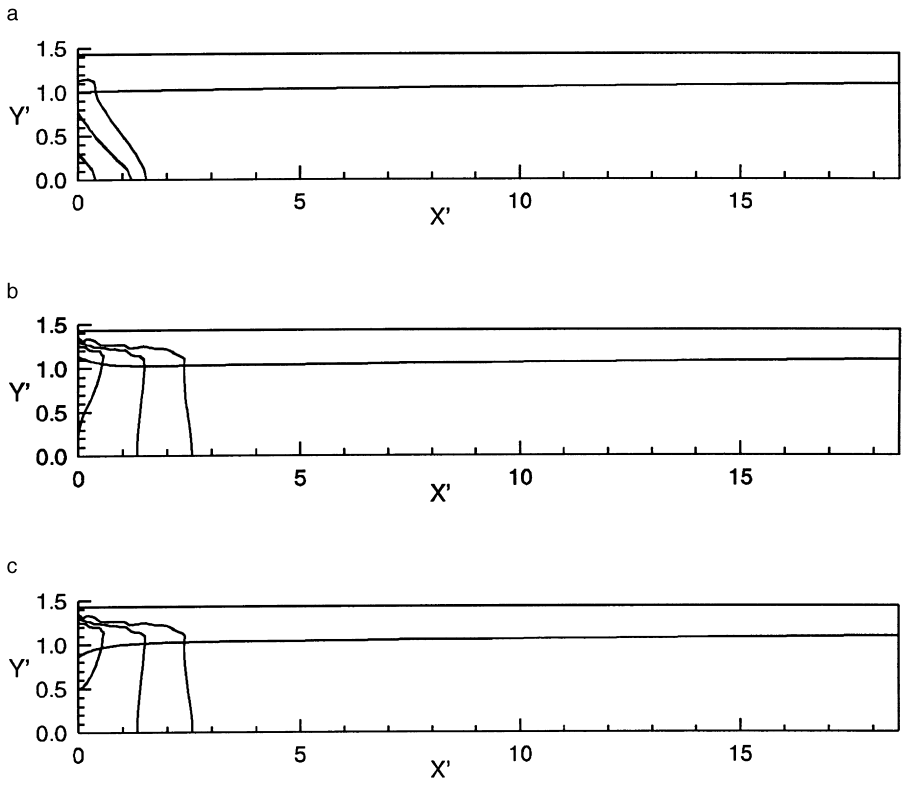

Fig. 12. (a) Steady-state, (b) high tide and (c) low tide water tables and salt concentration contours, 0.1, 0.5 and 0.9, for the case where the landward boundary condition is a constant head of 7.65 m (equivalent to 0.005 hydraulic gradient at steady-state condition).

This head is equivalent to a 0.005 hydraulic gradient. The salt concentration distributions for this case are shown in Fig. 10 along with the results for the case with flux boundary condition and 0.005 hydraulic gradient, where dotted and solid lines represent isochlor contours computed for head and flux boundary conditions, respectively. As explained before, in the case of the head boundary condition the sea-water intrudes further inland because of the reduction in the groundwater gradient caused by the water table over-height near the shoreline. In Fig. 11 the water table for this case is shown at different stages of tidal cycle. In this case, as the water table is kept constant at the landward boundary, the groundwater gradient is reduced.

The over-height introduced by tidal activity neglecting density differences is less for steep than for mild sloping beaches. To investigate the effect of beach slope on this process, a vertical face aquifer is considered. The aquifer is 130 m long, which is the horizontal distance between the land boundary and the intersection of the sea with the shoreline in the case of the sloping face aquifer. The other parameters are the same as in the basic problem. The landward boundary condition is the constant head of 7.65 m.

For this case, steady-state and transient salt concentration distributions are shown in Fig. 12. If the steady-state results for this case are compared with the corresponding case in Fig. 3, it can be seen that for the vertical beach slope the sea water has intruded a little further inland than for the sloping beach case. For example, the 0.1 contour toe is $1.571h_s$ and $1.429h_s$ distant from the intersection of the sea with the shoreline for the vertical and sloping face aquifers, respectively. In practical terms this difference is unlikely to be significant. As expected tidal fluctuations result in a more dispersed interface for the aquifer with a vertical face also. If the salt distribution contours for the vertical face are compared with those for the sloping beach, it can be seen that the salt water has intruded further inland for the sloping case. For example the 0.1 contour toe is about $2.571h_s$ and $3.857h_s$ distant from the intersection of the sea with the shoreline for the vertical and sloping face aquifers, respectively. As has been mentioned, this is partly because of the smaller over-height in the water table caused by tidal fluctuations with the vertical face. It is also because, in the case of a sloping beach, the salt-water can easily move inland over the sloping beach at the high tide stage and then infiltrate to the top of the aquifer.

6. Conclusions

A variable-density groundwater model is used to analyse the effects of tidal fluctuations on sea-water intrusion in an unconfined aquifer.

It is shown that the tidal activity forces the sea-water to intrude further inland and it also creates a thicker interface than would occur without tidal effects. Moreover, the configuration of the interface is radically changed when the tidal fluctuations are included. This is because of the dramatic changes in the flow pattern and velocity of the groundwater near the shoreline. For aquifer depths much larger than tidal amplitudes, the tidal fluctuation does not have much effect on how far the sea-water intrudes into the aquifer. However a significant change in the configuration of contours caused by the effect of tidal fluctuations is observed. The changes in the configuration of concentration contours caused by the tidal activity are more noticeable at the top of the aquifer, near to the water table, than at the bottom of the aquifer. This is caused by the infiltration of salt water into the top of the aquifer at higher tidal levels, and therefore a flatter beach slope intensifies this phenomenon. The interface configurations do not change noticeably over the course of a tidal cycle. Moreover, neglecting tidal fluctuation effects results in an inaccurate evaluation of the water table elevation at the land end of the aquifer, although little difference is seen between the water tables near the shoreline.

The results of the cases without tidal fluctuations confirm the previous results of Volker and Rushton (1982) for a confined aquifer that the seaward fresh-water flux in the aquifer has a considerable influence on both the shape and the location of the fresh-water to sea-water interface. It was shown that less fresh-water discharged to the sea not only causes the seawater to intrude further inland but also causes the occupied space between 0.1 and 0.9 contours to increase. In other words, it makes the interface more dispersed.

In the case where the landward boundary condition is a constant head the effects of tidal fluctuations on

sea-water intrusion are more pronounced than for cases where the landward boundary condition is a specified flux. In the latter case the over-height caused by tidal fluctuations reduces the overall hydraulic gradient.

The effects of tidal fluctuations are more significant for a sloping beach than for a vertical face and the salt water intrudes further inland for the sloping case. This is because of the smaller over-height in the groundwater table caused by tidal fluctuations at the vertical face and, because in the case of the sloping beach, the salt-water can easily move inland over the beach at the high tide stage and then infiltrate vertically through the top of the aquifer.

In general from a practical point of view, neglecting the effects of tidal fluctuations is non-conservative for the assessment of groundwater quality near the shore. For example, for a pumping well near the shore, the danger of seawater upconing would be increased. This is especially so for shallow aquifers exposed to large amplitude tides, as the tidal fluctuations force the seawater to intrude further inland and also create a thicker interface than would occur without tidal effects. As seen in Fig. 9 the distance from the intersection of the sea with the shoreline to the 0.1 contour toe has increased by about $1.0h_s$, $0.5h_s$, and $0.1h_s$, caused by the tidal influence for the normalised tidal amplitude of 0.143, 0.071, and 0.036 respectively.

Acknowledgements

The postgraduate scholarship of the Ministry of Culture and Higher Education of the Islamic Republic of Iran is appreciated. Financial assistance was provided partly by the Australian Research Council through a large grant for Coastal Groundwater Dynamics.

References

Ataie-Ashtiani, B., 1998. Contaminant transport in coastal aquifers. Ph.D. Thesis, Depart. Of Civil Eng. University of Queenland, Australia.

Bear, J., 1979. Hydraulics of groundwater, McGraw-Hill.

Celia, M.A., Bouloutas, E.T., Zarba, R.L., 1990. A general mass-conservative numerical solution for the unsaturated flow equation. Water Resour. Res. 26 (7), 1483–1496.

Custodio, E., 1988. Present state of coastal aquifer modelling: Short review. In: Custodio, E. Gurgui, A. Lobo Ferreira, J.P. (Eds.),Groundwater Flow and Quality Modelling. NATO ASI Series, vol. 224, Reidel, Dordrecht, pp. 785–810.

Elder, J.W., 1967. Transient convection in a porous medium. J. Fluid Mech. 27 (3), 609–623.

Fang, C.S., Wang, S.N., Harrison, W., 1972. Groundwater flow in a sandy tidal beach: two dimensional finite element analysis. Water Resour. Res. 8, 121–128.

Frind, E.O., 1982. Seawater intrusion in continuous coastal aquifer–aquitard systems. Adv. Water Resources 5, 89–97.

Glover, R.E., 1959. The pattern of fresh-water flow in a coastal aquifer. J. Geophys. Res. 64 (4), 457–459.

Hogan, P., 1988. Modeling of freshwater–seawater interaction on Enjebi Island, Enewetak Atoll. M.Sc. thesis, San Jose Univ. CA.

Inouchi, K., Kishi, Y., Kakinuma, T., 1990. The motion of coastal groundwater in response to the tide. J. Hydrol. 115, 165–191.

Konikow, L.F., Arevalo, J.R., 1993. Advection and diffusion in a variable-salinity confining layer. Water Resour. Res. 29 (8), 2747–2761.

Ledoux, E., Sauvagnac, S., Rivera, A., 1990. A compatible single-phase/two-phase numerical model: 1. Modeling the transient salt-water/fresh-water interface motion. Ground Water 28(1).

Li, L., Barry, D.A., Pattiaratchi, C.B., 1997. Numerical modelling of tidal-induced beach water table fluctuations. Coastal Engineering 30, 105–123.

Mercer, J.W., Larson, S.P., Faust, C.R., 1980. Simulation of salt-water interface motion. Ground Water 18 (4), 374–385.

Nielsen, P., 1990. Tidal dynamics of the watertable in beaches. Water Resour. Res. 26 (9), 2127–2134.

Philip, J.R., 1973. Periodic non-linear diffusion: An integral relation and its physical consequences. Aust. J. Phys. 26, 513–519.

Polo, J.F., Ramos Ramis, F.J., 1983. Simulation of salt water-fresh water interface motion. Water Resour. Res. 19 (1), 61–68.

Reilly, T.E., Goodman, A.S., 1985. Quantitative analysis of salt-water–freshwater relationships in groundwater systems- A historical perspective. J. Hydrol. 80, 125–160.

Segol, G., Pinder, G.F., Gray, W.G., 1975. A Galerkin-finite element technique for calculating he transient position of salt-water front. Water Resour. Res. 11(2).

Smiles, D.E., Stokes, A.N., 1976. Periodic solutions of a nonlinear diffusion equation used in groundwater flow theory: Examination using a Hele-Shaw model. J. Hydrol. 31, 27–35.

Taigbenu, A.E., Liggett, J.A., Cheng, A.H.-D., 1984. Boundary integral solution to seawater intrusion into coastal aquifers. Water Resour. Res. 20 (8), 1150–1158.

Underwood, M.R., Peterson, F.L., Voss, C.L., 1992. Groundwater tens dynamics of atoll islands. Water Resour. Res. 28 (11), 2889–2902.

Van Genuchten, M.Th., 1980. A closed-form equation for predicting the hydraulic conductivity of unsaturated soils. Soil Soc. Am. J. 44, 892–898.

Vauclin, M., Vachaud, G., Khanji, J., 1975. Two dimensional numerical analysis of transient waTer transfer in saturated–unsaturated soils, Computer Simulation of Water Resources Systems. In: Vansteenkiste, G.C.(Ed.), Proceeding of the IFIP working conference. North-Holland, Amsterdam, pp. 299–323.

Volker, R.E., 1980. Predicting the movement of seawater into a coastal aquifer. Tech. Pap. 51, Aust. Water Resour.

Counc. Dept. of Natl. Devel. Energy, Aust. Gov. Publ. Serv. Canberra.

Volker, R.E., Rushton, K.R., 1982. An assessment of importance of some parameters for seawater intrusion in aquifers and a comparison of dispersive and sharp-interface modelling approaches. J. Hydrol. 56, 239–250.

Volker, R.E., Ataie-Ashtiani, B., Lockington, D.A., 1997. Groundwater behaviour in tidal beaches. In: Proceedings of the 27th Congress of the International Association for Hydraulic Research. Pp. 511–517.

Voss, C.I., 1984. SUTRA: A finite-element simulation model for saturated–unsaturated fluid-density-dependent ground-water flow with energy transport or chemically-reactive single-species solute transport. U.S. Geol. Surv. Water Resour. Invest. Rep. 84-4369, p. 409.

Voss, C.I., Souza, W.R., 1987. Variable density flow and solute transport simulation of regional aquifers containing a narrow freshwater–saltwater transition zone. Water Resour. Res. 23 (10), 1851–1866.